Available online at www.sciencedirect.com
SCIENCE DIRECT®
Journal of Sound and Vibration 271 (2004) 391–410
JOURNAL OF SOUND AND VIBRATION
www.elsevier.com/locate/jsvi

Instability of systems with a frictional point contact. Part 2: model extensions

P. Duffour, J. Woodhouse*

Department of Engineering, University of Cambridge, Trumpington Street, Cambridge CB2 1PZ, UK

Received 16 July 2002; accepted 24 February 2003

Abstract

In a companion paper, a theory was presented which allows the study of the linear stability of a class of systems consisting of two subsystems coupled through a frictional contact point. A stability criterion in terms of transfer functions was derived and used to simulate the behaviour of generic systems. In the present paper, this approach was pursued and generalized by relaxing in turn certain of the assumptions made earlier. By doing this, it is possible to catalogue systematically all the routes to instability conceivable within the scope of linearity for the class of systems considered. The additional routes to instability identified are as follows. First, the contact point was made compliant by adding a linear contact spring at the interface between the two subsystems. This feature proved to have a significant influence on stability when the contact spring stiffness takes values of the same order of magnitude or lower than that of the average structural stiffness of the system. Second, a route to instability is possible if the system structural damping possesses a slight non-proportional component. The last and most elaborate extension consisted in allowing the coefficient of friction to vary linearly with the sliding speed. Simulation results suggest that a coefficient falling with increasing sliding speed can destabilize an otherwise stable system or can make it even more unstable. In accordance with previous results, a coefficient of friction rising with the sliding speed tends to make a system more stable, although this is not systematic. The theory presented here allows these possible routes to instability to be combined, so that data from vibration measurements or modelling and from frictional measurements can be used directly to predict the region of instability in parameter space.

1. Introduction

Many systems containing a sliding frictional contact of some kind are prone to self-excited vibration. Usually this is undesirable, as in squeal of vehicle brakes. Manufacturers of such

*Corresponding author. Fax: +44-1223-332662.
E-mail address: jw12@eng.cam.ac.uk (J. Woodhouse).

0022-460X/$ - see front matter
doi:10.1016/j.jsv.2003.02.004

systems would obviously like to be able to design them in such a way that squeal, judder, chatter or whatever it may be called does not occur. Such design efforts have up to now been based almost entirely on empirical modification and testing, but a rational design strategy based on a theoretical understanding of the phenomenon would be preferable. Although there is a long history of scientific literature on the subject, no fully satisfactory and well-validated general theory of frictional excitation of vibration has yet been demonstrated. In a companion paper [1], an attempt at the first stage of such a theory was advanced. Under certain assumptions, to be described in detail below, a method was presented which allows any frequencies of unstable vibration to be calculated from a knowledge of the vibration dynamics of the contacting systems, and the frictional conditions at the contact. This theoretical framework was used to analyse generic systems, to establish which features encourage or inhibit instability.

The goal of the research is to catalogue all possible "routes to instability" within a unified framework. It seems likely that there is no single phenomenon of brake squeal, or whatever: rather, there is a family of related but distinct mechanisms of instability. To design a non-squealing brake it is not sufficient to design against one particular form of instability while neglecting others. A robust design must take account of all possible instabilities. The earlier paper [1] considered a deliberately circumscribed family of systems, to establish the groundwork. In the present work certain of the assumptions made there will be relaxed, to see whether and when new forms of instability can appear. The intention is that this process will be continued in later work so that systems of increasing generality are drawn within the scope of the theory. In parallel, experimental studies are being made to test the predictions of the initial theory, and these will also be extended to progressively more complicated systems.

The theory proposed in [1] relies on the following set of assumptions:

1. The dynamics of the two subsystems in contact are *linear*.
2. The subsystems are in a *steady-sliding regime*.
3. Sliding results from the motion of one or both subsystems. The bulk motion of the moving subsystem(s) *does not alter significantly its/their dynamical properties* measured at rest.
4. Sliding occurs at a *single location with no geometrical extension* (single point contact).
5. The contact between the two subsystems is *not compliant*.
6. The *damping is proportional* so that the modes of the two subsystems can be described by real mode shape coefficients.
7. The relation between the friction force and the normal force can be appropriately described by *a constant coefficient of friction*.

With these assumptions, two main conclusions were drawn. First, instability mainly occurs when sequences of three consecutive modes have displacements at the contact point with a particular pattern of signs. More precisely, instability is linked to the presence of modes such that the product of the tangential and normal mode shape coefficients is negative. When this occurs, a sufficiently high value of the coefficient of friction will produce the required sign pattern. For definiteness, the two contacting subsystems will be referred to as the "disc" and the "brake": if the disc is perfectly symmetrical, such modes can only originate from the brake subsystem. The second conclusion was that instability is more likely to arise if subsystem modes have very different damping factors.

The present paper investigates the stability of slightly more general systems, obtained by relaxing certain of the assumptions just listed. Some of these assumptions cannot be relaxed easily. For instance, allowing the dynamics to be non-linear (i.e., relaxing (1)) would change the nature of the problem profoundly and require a different style of analysis. This assumption will be retained throughout the present work.

Assumptions (2) and (3) can be empirically or practically motivated: squeal mainly occurs at very low speeds (which supports (3)) and in a vast majority of cases it indeed occurs in systems in steady sliding, for example when a disc or drum brake is applied to stop a vehicle.

Relaxing assumption (4) would be difficult if it is understood as implying line contact or area contact. However, it is possible to extend the theory of the companion paper [1] by reformulating the theory with two contact points. The algebra becomes more complex and the study of the stability will be the object of further research.

This leaves assumptions (5)–(7). These will be relaxed in turn: (5) and (6) are very easily dealt with, but (7) requires a more elaborate analysis. For each assumption relaxed, a revised stability criterion will be derived and investigated by simulating the behaviour of generic systems.

Relaxing assumption (5). The system studied in [1] can be modified by allowing the contact to be compliant. Extending the theory to include this feature was also motivated by reports from researchers studying brake noise using the finite element method (e.g., [2]). They observed that adding a contact spring between the contacting nodes can have a strong influence on the stability. Using standard linear system techniques, the system studied in [1] was modified by adding a contact spring at the interface of the two subsystems. A modified version of the stability criterion can be derived using standard linear system techniques and its significance investigated.

Relaxing assumption (6). The second extension investigated is the non-proportionality of the structural damping. To our knowledge, this has never been mentioned as a possible source of instability in friction-induced vibration studies. However, if the structural damping is non-proportional, transfer functions take a slightly different form and it will be shown that this can affect the stability of the system in an unexpected way.

Relaxing assumption (7). In the companion paper, the stability criterion was derived by modelling the contact interaction by a constant coefficient of friction. In the present work, this assumption will be relaxed and the coefficient of friction will be allowed to vary. A coefficient of friction decreasing with the sliding speed was long thought to be the main source of friction-induced vibration. It is now generally agreed that this is not the only cause of instability, but the influence of velocity-dependent friction is still of interest. For definiteness, the theory will be presented for a coefficient of friction varying linearly with the sliding speed. However, it will be seen that many other friction laws, once linearized, would take a similar form, so that the conclusions can apply to a rather general class of frictional interactions.

2. Influence of contact compliance

Before studying how contact compliance influences stability calculations, it is useful to recall the basics of Hertz theory, since it is within this framework that the notion of contact stiffness is best defined [3].

2.1. Background of contact compliance

Assuming that a single spherical asperity made of a linearly elastic material is pressed on a rigid smooth flat plane, Hertz showed that the normal compliance law takes the form:

$$N = A\delta^{3/2}, \tag{1}$$

where N is the normal load, A is a coefficient of proportionality depending on the geometry and the mechanical properties of the sphere, and δ is the surface separation. Thus, Hertz' theory predicts a non-linear normal compliance law. For small dynamic variations of load around a mean value, this law can be linearized around the operating load value. The contact stiffness can then be defined as the coefficient of proportionality between N and δ in this linearized law. The generalization of such a law to extended areas of contact between rough surfaces is a difficult problem. In general, a statistical characterization of the surfaces is necessary. Greenwood and Williamson [4] gave a solution assuming a Gaussian peak height distribution and showed how it gives rise to the familiar Coulomb law of friction. However, throughout this paper, a point contact is assumed so the issue of distributed contact does not arise.

Some authors have suggested that contact compliance may have an effect on the stability of systems in sliding contact. Interest in this area actually stems from two different concerns. The first originates from a seminal paper by Tolstoï [5], in which it was suggested that there is no essential difference between kinematic and static friction. The apparent distinction is due to the influence of normal vibration superimposed on the tangential vibration. A number of authors [6–8] have developed this idea further. If the normal contact compliance is non-linear, of Hertz type, the waveform of normal oscillations will be significantly non-symmetrical and such that the average "dynamic penetration" of the contacting surfaces will be smaller than the static "penetration". This would produce a slight lifting-up of the slider, which in turn results in a reduction of the real contact area, thus reducing the coefficient of friction. This mechanism explains how a non-linear contact compliance can result in an apparent drop in the friction coefficient in a dynamic regime. For more detail see [6, pp. 36–38]. However, this mechanism lies outside the linearized theory relevant to this study.

The second interest in contact compliance in relation to friction instability is more relevant here and arises from its use as a convenient device in computational studies. When a brake assembly, for instance, is modelled by finite elements, it is convenient to include contact springs between contacting nodes. By this device, the normal contact force is simply the product of the contact spring stiffness and the node distance. The friction force is then obtained by multiplying the normal force and the coefficient of friction [2,9,10]. A sufficiently large value for this contact stiffness (typically 10^6 N/m) also ensures that the surfaces in contact do not penetrate. Within this context, the contact stiffness becomes a parameter which can be varied like any other and it is possible to investigate its influence on stability.

2.2. Addition of a contact stiffness to the linear model

Adding a linear contact spring between the two subsystems poses no difficulty for the model presented in [1].

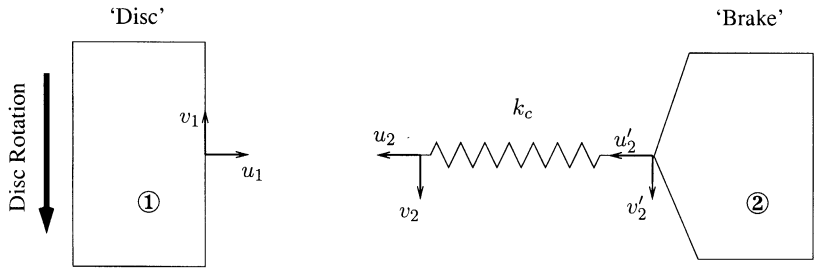

Fig. 1. Diagram showing two linear systems in sliding contact through a contact spring. u_i and v_i denote, respectively, the tangential and normal displacements at the location shown.

In Fig. 1, a normal contact spring k_n has been included at the tip of the "brake". This spring could equally well have been attached to the disc, or two different contact springs could even be attached at the contacting end of each subsystem. u_2' and v_2' represent the displacement of the brake tip in the direction shown, while u_2 and v_2 represent the displacement at the end of the contact spring that will now be in contact with the disc. For clarity, the forces are not represented on this picture. With the same notations and sign conventions used in [1], there are equal and opposite normal and tangential forces N and F at the new contact point. Each force is decomposed into a static component, denoted with a zero subscript, and a fluctuating component denoted with a prime. These forces are transmitted directly through the massless spring. The dynamics of the two subsystems "disc" and "brake" considered independently are again represented using the matrices of transfer functions previously defined. If the contact region is compliant in the normal direction and if that compliance matters for stability, there is no reason to believe that the same will not be true in the tangential direction [11–13]. Therefore, a contact spring in the tangential direction k_t will also be included in the analysis, although this is not shown in Fig. 1 to prevent overloading.

For clarity, the notation used to express these transfer functions in [1] is recalled in Table 1.

Following Soedel [14] or Bishop and Johnson [15], the contact springs and the "brake" can be viewed as two linear systems in series. The relationships among forces and displacements defined in Fig. 1 are

$$N' = k_n(u_2 - u_2') = k_n(u_2 - H_{11}N' - H_{12}F'), \tag{2}$$

$$F' = k_t(v_2 - v_2') = k_t(v_2 - H_{21}N' - H_{22}F'). \tag{3}$$

The dynamics of the subsystem "brake" coupled with the contact springs can then be expressed from the new contact point via the matrix $\mathbf{H}'$ defined as

$$\begin{bmatrix} u_2 \\ v_2 \end{bmatrix} = [\mathbf{H}'] \begin{bmatrix} N' \\ F' \end{bmatrix} = \begin{bmatrix} H_{11}(\omega) + \dfrac{1}{k_n} & H_{12}(\omega) \\ H_{21}(\omega) & H_{22}(\omega) + \dfrac{1}{k_t} \end{bmatrix} \begin{bmatrix} N' \\ F' \end{bmatrix}. \tag{4}$$

In this formulation, it is assumed that the contact compliance does not induce any cross-coupling term between the normal and tangential directions. With $\mathbf{H}'$ thus defined, the process outlined in the companion paper [1] can be applied in exactly the same way. Assuming a constant coefficient

Table 1
Expression of the transfer functions for the brake and the disc

Disc	Brake
$G_{11}(\omega) = \sum_n \frac{\phi_n^2(x)}{\omega_n^{d2} + 2i\omega\omega_n^d\delta_n^d - \omega^2}$	$H_{11}(\omega) = \sum_n \frac{\psi_n^2(x)}{\omega_n^{b2} + 2i\omega\omega_n^b\delta_n^b - \omega^2}$
$G_{12}(\omega) = \sum_n \frac{\phi_n(x)\phi_n(y)}{\omega_n^{d2} + 2i\omega\omega_n^d\delta_n^d - \omega^2}$	$H_{12}(\omega) = \sum_n \frac{\psi_n(x)\psi_n(y)}{\omega_n^{b2} + 2i\omega\omega_n^b\delta_n^b - \omega^2}$
$G_{22}(\omega) = \sum_n \frac{\phi_n^2(y)}{\omega_n^{d2} + 2i\omega\omega_n^d\delta_n^d - \omega^2}$	$H_{22}(\omega) = \sum_n \frac{\psi_n^2(y)}{\omega_n^{b2} + 2i\omega\omega_n^b\delta_n^b - \omega^2}$

of friction, the conclusion is now that the fully coupled system is unstable if and only if the function

$$D(\omega) = \frac{1}{k_n} + \frac{1}{k_t} + G_{11} + \mu_0 G_{12} + H_{11} + \mu_0 H_{12} \tag{5}$$

has at least one zero in the lower half complex ω-plane. Before investigating the effect of the extra term from simulation results, some general comments can be made.

First, it appears from Eq. (5) that the normal and tangential compliances have an equivalent influence on stability. This justifies the assumption that if a normal spring is included, a tangential one should too.

It is also interesting to examine how the contact stiffness term alters the expected number of zeros of D. Assuming proportional damping, as in Table 1, $D(\omega)$ can again be expressed in terms of the real mode shapes, natural frequencies and damping factors of the two uncoupled subsystems. This yields the following expression for $D(\omega)$:

$$D(\omega) = \frac{1}{k_n} + \frac{1}{k_t} + \sum_i \frac{\phi_i^2(x)}{(\omega_i^{d2} + 2i\omega\omega_i^d\delta_i^d - \omega^2)} + \sum_i \frac{\psi_i(x)[\psi_i(x) + \mu_0\psi_i(y)]}{(\omega_i^{b2} + 2i\omega\omega_i^b\delta_i^b - \omega^2)}. \tag{6}$$

As in [1], the mode shape combinations in the numerator of each resonant term will be called a_1, a_2, etc. When the contact stiffnesses are not included, it was shown in [1] that a system containing N modes in total when the subsystems are uncoupled possesses $N-1$ modes once the subsystems are coupled. Now, the same initial N modes give a total of N modes for the coupled system, as can be seen by putting the terms in D to the same denominator. If both positive and negative frequency poles are included in the analysis, this indicates that an extra pair of complex conjugate zeros has appeared, intuitively representing the ''contact resonance''. The reason is that the two ''masses'' at the original contacting points are no longer merged into a single ''mass'' but remain as separate degrees of freedom.

Another point deserves some discussion. In [1], the absolute magnitude of values given to the mode shape compounds a_i was not a problem. The expression for $D(\omega)$ was a linear combination of the a_i, therefore only their relative sign and magnitude mattered. In this section, however, the addition of a constant stiffness term introduces an 'absolute' reference in terms of magnitude. It is

useful to carry out a simple order of magnitude analysis in order to estimate plausible values to be used in the subsequent simulations. Assuming that 1 kg is a plausible value for the modal mass of a typical brake system, then, to a normalized natural frequency of 1, corresponds a non-dimensional structural stiffness of order unity too. Thus, the values chosen for the contact stiffness in the following simulations will have to be consistent with a structural stiffness of order unity.

2.3. Simulation results

Some simulation results will now be described. For ease of comparisons and connections with previous results, a contact compliance is added to the three-mode system investigated in [1, Section 4.3].

Fig. 2 shows two surface plots of the minimum imaginary part of the zeros for systems consisting of three modes plus contact compliance, characterized by the "equivalent" contact stiffness $k_e = k_t k_n/(k_t + k_n)$. The two plots correspond to two different values of k_e: (a) $k_e = 10$ and (b) $k_e = 0.1$. Amongst the three modes constituting the system, two are fixed with frequencies 1 and 1.2, damping factors 0.01, 0.01 and both amplitudes equal to 1 (by "amplitude" is meant the numerator coefficient of the corresponding term in Eq. (6)). The third mode is varied in frequency within 0.8 and 1.4, and in amplitude within -5 and 0. Its damping factor is set to 0.03. Following the notation defined in [1], the natural frequency and amplitude of the varying third mode will be denoted ω_3 and a_3 respectively. On each surface plot, the zero contour is plotted with a thick line on the surface itself, as well as on the bottom plane. As before, the minimum imaginary part is taken among those roots whose real part lies within the range of validity [0.6 1.6].

Fig. 2 clearly shows that $k_e = 1$ is indeed a critical value. In Fig. 2(a), where $k_e = 10$, the surface plot looks very similar to the corresponding plot obtained in [1] for the same underlying three-mode system, without contact springs. For this value of k_e, the main effect of the contact compliance is to initiate a steep "canyon" spanning the higher range of the third mode frequency and approximately centred on the line $a_3 = -2.5$. This canyon becomes wider and wider as k_e

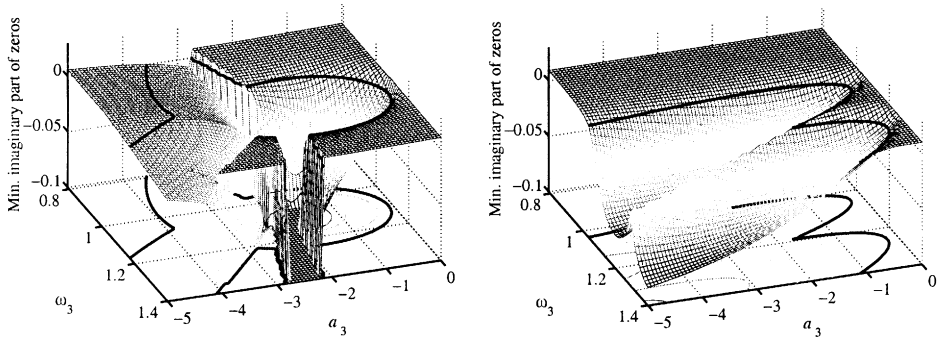

(a) $k_e = 10$ (b) $k_e = 0.1$

Fig. 2. Surface plots showing the minimum imaginary part of the zeros for systems consisting of three modes and a contact frequency term varied as shown. Two of the modes are fixed, while the third one is varying in frequency and amplitude. The bottom of these plots has been clipped at 0.1 to make important features more visible. The thick line plotted on the surface is the zero contour. This contour is also reproduced on the bottom plane.

decreases, gradually deforming the higher quadrant of the surface plot (larger values of ω_3 and $|a_3|$). This can be seen in Fig. 2(b). Note that the half of the surface corresponding to the lower frequency range is little affected, even for small values of k_e. As k_e becomes larger, the width of the canyon reduces, so that for $k_e = 100$ (case not shown), the surface plot looks almost as if the contact was not compliant (i.e., as if the contact spring had an infinite stiffness). This is not surprising since k_e only affects the function $D(\omega)$ through its inverse $1/k_e$, so that relatively large values of k_e will only have a slight effect on the stability.

Fig. 2(b) shows that lower values of the contact stiffness k_e significantly modify the behaviour of the underlying three-mode system. This plot also shows that such values can significantly increase the region in which the system is unstable. It seems that, as the value of k_e becomes smaller, two "dips", characteristic of a three-mode cluster with alternating signs, lie next to each other. This similarity is not fortuitous. In [1, Section 4.2], the influence of remote poles was modelled as a constant residual. It was argued that far away from a mode natural frequency, the influence of this mode on $D(\omega)$ could be modelled as a *real constant*. Mathematically, this is precisely what the contact stiffness term in Eq. (5) amounts to. Therefore, it is not surprising that the influence of a compliant contact bears a strong similarity with the influence of a remote mode. As the equivalent contact stiffness k_e becomes smaller, its inverse increases in magnitude. So, one might not expect this similarity to continue to hold, since the approximation of a neighbouring mode by a constant residual term may no longer be accurate. However, simulation results (not shown for lack of space) suggest that a contact stiffness has a strikingly similar effect to that of a remote mode, even for relatively low stiffness values. This is a quite remarkable result.

2.4. Conclusions on the influence of contact compliance

In this section, a contact compliance was added to the linear formulation presented in the companion paper [1]. This compliance was modelled by tangential and normal linear springs. A new expression for the function $D(\omega)$ governing the stability of the coupled system was obtained. Simulated examples showed that a contact compliance significantly affects the system stability when the value of the contact stiffness is of the same order or below the order of magnitude of the structural stiffness. If the contact stiffness takes a value of this order of magnitude, then, to a good approximation, the effect on the system is similar to that of a remote extra mode.

3. Influence of non-proportional damping and complex modes

If the damping in either or both subsystems is not extremely small, there is another effect which can influence the threshold of stability. So far, proportional damping has been assumed throughout the system, so that the mode shapes are real. However, although this assumption is very commonly made, the condition of proportional damping is an artificial one, made purely for mathematical convenience. There is no physical reason to expect most real systems to conform to this assumption. Instead, one must expect mode shapes to be complex in general. For most purposes of vibration modelling this distinction matters little, but for stability analysis it can be very important since it introduces phase shifts. Unfortunately, there is no universal predictive theory of structural damping which has the same convincing physical justification as the treatment

of stiffness and inertia through stiffness and mass matrices. The best that can be said is that if the damping is governed by linear theory and is light, then a perturbation approach can be used to obtain approximations to the complex frequencies and mode shapes. Surprisingly, it turns out that the expressions for transfer functions are closely analogous to those used before. Specifically, expansions like those in Table 1 take approximately the same form, provided the mode shapes appearing in the coefficients are replaced by their approximate complex equivalents [16].

It is not usually possible to predict the complex mode shapes from an a priori model of a system, but at least it is possible to measure them. The techniques of experimental modal analysis can be applied in the standard way [17], and provided a sufficiently sophisticated signal-processing method is used, complex mode shapes can be extracted.

It is of interest to examine briefly the effect of complex mode shapes on the threshold of stability. In this particular context, the important physical interpretation of complex mode shapes is simply that, in a mode of the 'brake', the normal and tangential components of motion might not be exactly in phase. In a free vibration, the contact point would then describe an elliptical path rather than oscillating along a straight line. For the generic systems studied here, the introduction of even slightly complex modes can have a very significant effect. This effect can be better understood if the expected number of zeros is first considered. Suppose there are N poles at positive frequencies and correspondingly N negative frequencies. Multiply out the partial fraction expansion into a ratio of polynomials. If the damping is not proportional, so that the residues are complex, the numerator polynomial will have $(2N-1)$ zeros. However, if the damping is proportional, the order turns out to be only $(2N-2)$ [1]. This means that with non-proportional damping, an extra single zero must appear, and on symmetry grounds this must lie on the imaginary axis since the numerator of $D(\mathrm{i}\omega)$ is a real-valued polynomial. As an infinitesimal imaginary part is added to one of the residues, this new zero appears "from infinity", either at very large positive values or at very large negative values depending on the sign of the imaginary part of the residue. To see this behaviour algebraically, it is enough to consider just one pair of poles. Using the notation defined in [1],

$$D = \frac{c_1}{(\omega - \bar{\omega}_1)} - \frac{c_1^*}{(\omega + \bar{\omega}_1^*)} = \frac{(c_1 - c_1^*)\omega + c_1\bar{\omega}_1^* + c_1^*\bar{\omega}_1}{(\omega - \bar{\omega}_1)(\omega + \bar{\omega}_1^*)}, \tag{7}$$

where the star denotes complex conjugation. This function has a single zero, at

$$\omega_z = \mathrm{i}\,\frac{\mathrm{Re}(c_1\bar{\omega}_1^*)}{\mathrm{Im}(c_1)}. \tag{8}$$

As $\mathrm{Im}(c_1)$ tends to zero this moves off along the imaginary axis to infinity, the direction (and hence stability) depending on the sign of the ratio in Eq. (8).

This result is quite unexpected: a very small amount of non-proportional damping, if it induces a complex residue with the appropriate sign, can immediately produce a very strong instability in a system which was previously stable. In [1, Section 4.3], purely imaginary zeros were also predicted for some parameter values, even with real residues. It was then argued that these zeros should not be given too much significance since the analysis was only intended to be locally valid, and they fall outside the range of validity of the model. The situation is now slightly different: however many modes are included in the model, if the residues become complex, a purely imaginary zero will appear, stable or unstable depending on the other parameter values.

Therefore, an assumption of proportional damping could be dangerously misleading in any study of the stability of frictionally sliding systems. It seems plausible that this phenomenon is giving one more clue regarding the physical mechanisms underlying 'capriciousness', since small changes to a system might influence the (slight) complexity of the modes. This conclusion, together with those of the companion paper [1] regarding the influence of damping point towards the crucial importance of modelling damping accurately, if one hopes to make reliable stability predictions for friction-induced vibration.

4. Influence of varying coefficient of friction

In this section, the influence of a coefficient of friction varying with sliding speed is investigated. It is well known that including such a feature for a single-degree-of-freedom oscillator introduces a term proportional to the velocity into the equation of motion. A coefficient of friction decreasing with increasing sliding speed (negative resistance) has often been proposed as a possible mechanism for frictional instability (e.g. [18]). Within the scope of a linearized theory, it is possible to use a friction law featuring such a variable coefficient of friction. First, a new stability criterion including this friction law is derived.

4.1. Solution with a variable coefficient of friction

It is a common observation from frictional tests carried out at different speeds of steady sliding that the coefficient of friction may vary, either increasing or decreasing as sliding speed increases. If this variation carries over to high-frequency dynamic variations of speed and friction force, then the relation in the vicinity of the imposed sliding speed from the disc rotation can be linearized, so that

$$F \approx [\mu_0 + \mathrm{i}\omega\varepsilon(v_1 + v_2)]N, \tag{9}$$

hence

$$F_0 + F' \approx [\mu_0 + \mathrm{i}\omega\varepsilon(v_1 + v_2)](N_0 + N') \tag{10}$$

$$\approx \mu_0 N_0 + \mathrm{i}\omega\varepsilon N_0(v_1 + v_2) + \mu_0 N' \tag{11}$$

so that

$$F' \approx \mathrm{i}\omega\varepsilon N_0(v_1 + v_2) + \mu_0 N'. \tag{12}$$

The factor $\mathrm{i}\omega$ serves to convert the displacements v_1 and v_2 into velocities. ε denotes the slope of the straight line characterizing the linear relation between F and v.

When the system is analysed using the more general friction law (12) the expressions presented in Section 2 of [1] become more complicated. Using the notation introduced in [1],

$$v_1 + v_2 = \left[\frac{G_{12} + \mu_0 G_{22} + H_{12} + \mu_0 H_{22}}{1 - \mathrm{i}\omega\varepsilon N_0\ (G_{22} + H_{22})}\right] N' = K(\omega)N' \tag{13}$$

say. Then, one has

$$N' = \frac{r}{D(\omega) + \mathrm{i}\omega\varepsilon N_0\ (G_{12} + H_{12})K(\omega)} \tag{14}$$

so that, for example

$$u_1 = \frac{G_{11} + \mu_0 G_{12} + \mathrm{i}\omega\varepsilon N_0[G_{12}(G_{12} + H_{12}) - G_{11}(G_{22} + H_{22})]}{D(\omega) - \mathrm{i}\omega\varepsilon N_0\ [(G_{11} + H_{11})(G_{22} + H_{22}) - (G_{12} + H_{12})^2]} r. \tag{15}$$

The numerator of this expression consists of transfer functions of stable systems, and contains no unstable poles. Thus the new condition for instability is that the function

$$\begin{aligned} E(\omega) &= D(\omega) - \mathrm{i}\omega\varepsilon N_0\ [(G_{11} + H_{11})(G_{22} + H_{22}) - (G_{12} + H_{12})^2] \\ &= D(\omega) - \mathrm{i}\omega\varepsilon N_0 \det[\mathbf{G} + \mathbf{H}] \end{aligned} \tag{16}$$

has at least one zero in the lower half-plane, where **G** and **H** denote the transfer function matrices previously defined.

The effect of the more complicated linearized friction law equation (12) will be examined using simulated examples. Following the earlier presentation of the constant coefficient of friction case, the next section gathers some general points that can be made from inspection of the criterion just derived. Many of these points will be useful when the behaviour of the system is later simulated.

4.2. General comments on the new criterion

4.2.1. Miscellaneous remarks

(1) First, criterion (16) reassuringly reduces to the previous condition (Eq. (7) in [1]) when $\varepsilon = 0$.

(2) From the sign conventions of Fig. 1, $(v_1 + v_2)$ is *minus* the change in sliding speed due to the vibration, so that a positive value of ε corresponds to a friction coefficient which decreases with increasing sliding speed; precisely the condition which commonly produces an effect of "negative resistance" (e.g. [19]).

(3) When the coefficient of friction is allowed to vary with the sliding speed, the stability of the system appears to be influenced by the static value of the normal load N_0. This is a new feature: so far, only the fluctuating quantities had an effect. Eq. (16) also shows that mathematically ε has the same effect as the nominal normal load N_0. It is very difficult to know a priori which values these two parameters should take for a typical system. For convenience, they will often be treated as a single compound quantity in the simulation section.

4.2.2. Expression of $E(\omega)$ in terms of modal parameters

Proportional damping will be assumed so that the standard transfer function formulae can be used. The disc will again be supposed to be perfectly axisymmetrical, so that $G_{12} = G_{21} = 0$. In contrast to the companion paper [1], G_{22} appears in the stability criterion. This raises an issue. The symmetry argument adduced to conclude that $G_{12} = 0$, implies that $\phi_n(x)\phi_n(y) = 0$ for all disc modes. Clearly for out-of-plane disc modes, $\phi_n(x)$ is non-zero. One could then be tempted to conclude that $\phi_n(y) = 0$, which would imply that G_{22} is also be zero. This is obviously incorrect. The reason for this apparent contradiction lies in a subtlety of disc vibration which did not matter previously, but which it is now necessary to clarify. For modes of the disc which do not contain

any nodal diameter, $\phi_n(y)$ is zero, so that these modes do not contribute either to G_{12} or G_{22}. However, any mode with at least one nodal diameter will appear as a doublet. G_{11} is the normal response, at the contact point, to a normal impulse at the contact point. If the disc is perfect, a normal impulse will only excite one mode of each doublet, and this mode will have an antinode at the point of impact, so that lateral motion, corresponding to $\phi_n(y)$, cannot arise. Similarly, G_{22} is the lateral response at the contact point, to a lateral impulse at the contact point. This time, only the second mode of the doublet—that which has a nodal line at the contact point, will be excited, so that no normal motion arises at the contact point. Lateral motion is due to the thickness of the plate. This is illustrated in Fig. 3, with a three nodal diameter doublet.

It is now clear that both G_{11} and G_{22} really contribute to $E(\omega)$, although $G_{12} = 0$. This point clarified, it is possible to obtain an expression for $E(\omega)$ in terms of modal parameters. $E(\omega)$ being significantly more complicated than $D(\omega)$, it is difficult to obtain an expression for an indeterminate number of modes n. Therefore, the expanded form $E(\omega)$ will be derived first for a system consisting of three terms: two from the disc and one from the brake. Note that according to the explanation just given, this actually amounts to one mode of the brake and four modes of the disc in general, although there are only three resonant frequencies in all. The same procedure can be applied if more modes are included.

To simplify the notation, the quadratic denominators appearing in the transfer functions recalled in Table 1 will be denoted $\mathscr{D}isc_1$, $\mathscr{D}isc_2$ for the disc, and $\mathscr{B}rake_1$ for the brake. With this notation:

$$\det[\mathbf{H}+\mathbf{G}] = \left(\frac{\phi_1^2(x)}{\mathscr{D}isc_1}+\frac{\phi_2^2(x)}{\mathscr{D}isc_2}+\frac{\psi_1^2(x)}{\mathscr{B}rake_1}\right)\left(\frac{\phi_1^2(y)}{\mathscr{D}isc_1}+\frac{\phi_2^2(y)}{\mathscr{D}isc_2}+\frac{\psi_1^2(y)}{\mathscr{B}rake_1}\right)-\frac{\psi_1^2(x)\psi_1^2(y)}{\mathscr{B}rake_1^2}. \tag{17}$$

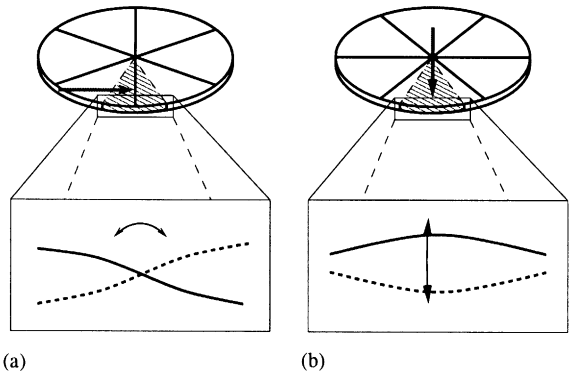

Fig. 3. Diagrams showing the vibration of a disc in a three-diameter mode when the disc is excited by a lateral impulse (a) or a normal impulse (b). The thick lines on the disc represent the nodal diameters. The thick arrows represent the impulses. The zoomed frames show the motion of the median plane of the disc. In case (a), there is a nodal line at the point of impact so that no out-of-plane motion is possible. Lateral motion arises through the thickness of the disc. In case (b), there is an anti-nodal line at the point of impact so that no lateral motion is generated along the anti-nodal diameter.

Expanding, the expression for $E(\omega)$ can be written:

$$E(\omega) = \frac{\phi_1^2(x)}{\mathscr{D}isc_1} + \frac{\phi_2^2(x)}{\mathscr{D}isc_2} + \frac{\psi_1(x)(\psi_1(x) + \mu_0\psi_1(y))}{\mathscr{B}rake_1} - \mathrm{i}\omega\varepsilon N_0 \left[\frac{\phi_1^2(x)\phi_1^2(y)}{\mathscr{D}isc_1^2} + \frac{\phi_2^2(x)\phi_2^2(y)}{\mathscr{D}isc_2^2} + \frac{\phi_2^2(x)\phi_1^2(y) + \phi_1^2(x)\phi_2^2(y)}{\mathscr{D}isc_1\mathscr{D}isc_2} + \frac{\phi_1^2(x)\psi_1^2(y) + \psi_1^2(x)\phi_1^2(y)}{\mathscr{D}isc_1\mathscr{B}rake_1} + \frac{\phi_2^2(x)\psi_1^2(y) + \psi_1^2(x)\phi_2^2(y)}{\mathscr{D}isc_2\mathscr{B}rake_1} \right]. \quad (18)$$

In Eq. (18), the first three terms correspond to the expression of $D(\omega)$ derived in the companion paper [1]. The remaining terms correspond to the expanded expression of the new determinantal term. The zeros of $E(\omega)$ are the zeros of the numerator of the single fraction obtained when all the terms in equation (18) are put to the same denominator. If $P_\varepsilon(\omega)$ denotes this polynomial numerator, its expression can be given by multiplying E by the common denominator:

$$P_\varepsilon(\omega) = E(\omega) \times \mathscr{D}isc_1^2 \times \mathscr{D}isc_2^2 \times \mathscr{B}rake_1 \times \mathscr{B}rake_2 = \underbrace{\phi_1^2(x)\mathscr{D}isc_1\mathscr{D}isc_2^2\mathscr{B}rake_1\mathscr{B}rake_2\ldots}_{D(\omega)} - \mathrm{i}\omega\varepsilon N_0 \underbrace{[\phi_1^2(x)\phi_1^2(y)\mathscr{D}isc_2^2\mathscr{B}rake_1\mathscr{B}rake_2\ldots]}_{\det[\mathbf{H}+\mathbf{G}]}. \quad (19)$$

The term introduced by the varying coefficient of friction, $\mathrm{i}\omega\varepsilon N_0\det[\mathbf{H}+\mathbf{G}]$, can be thought of as a *real* function of $\mathrm{i}\omega$, so that $P_\varepsilon(\mathrm{i}\omega)$ is also a real polynomial, and its roots will again be either purely imaginary or "i" times a complex conjugate pair. $P_\varepsilon(\mathrm{i}\omega)$ is a polynomial of degree 8, yielding four modes for the coupled system (if the zeros are all complex).

The generalization of expansion (18) is rather intricate, but some useful insight can be gained from understanding the process. Assume that the disc, considered independently, has N_d modes and the brake, N_b. A general expression for $D(\omega)$ was given in [1, Eq. (12)]. The same expression is still valid for the corresponding part in $E(\omega)$. The new, determinant term is more complicated. Each term in $\det[\mathbf{H}+\mathbf{G}]$ will have at the denominator a product of any two quadratics $\mathscr{D}isc_n$ and/or $\mathscr{B}rake_k$, except for the terms in $\mathscr{B}rake_k^2$, which cancel out in the determinant calculation. In general, there is no divisor common to all these denominators, so that to put the terms of E to the same denominator to obtain P_ε, it is necessary to multiply $E(\omega)$ by the product of all the disc quadratics squared, $\mathscr{D}isc_n^2$, multiplied by the product of all the brake quadratics $\mathscr{B}rake_k$ (not squared). This amounts to multiplying $E(\omega)$ by the product of all the denominators, which is a polynomial of degree $2\times(2N_d+N_b)$. At the denominator of each fractional term in $D(\omega)$, there is a single quadratic term $\mathscr{D}isc_n$ or $\mathscr{B}rake_k$. The denominators of the terms of $\det[\mathbf{H}+\mathbf{G}]$ involve the product of two quadratics. When E is multiplied by the product of quadratics as shown in Eq. (19), only one quadratic cancels out for each term of D, whereas two will simplify for each determinant term. It follows that each term of $D(\omega)$ yields a polynomial of degree $2\times(2N_d+N_b)-2$, whereas the terms coming from $\det[\mathbf{H}+\mathbf{G}]$ are polynomials of degree $2\times(2N_d+N_b)-4$. Due to the multiplication of the determinant by $\mathrm{i}\omega$, these polynomials become of degree $2\times(2N_d+N_b)-3$ and they have no constant term (i.e., coefficient of degree zero). This has several consequences:

- The degree of $P_\varepsilon(\omega)$ is the same as the degree of the polynomials coming from $D(\omega)$, that is, $2\times(2N_d+N_b-1)$. By comparison, the corresponding degree of $P(\omega)$, when the coefficient of

friction is constant, is $2 \times (N_d + N_b - 1)$. The new factor 2 multiplying N_d is related to the presence of doublet modes.

- The term of highest power of $P_\varepsilon(\omega)$ will come from $D(\omega)$ and the leading coefficient (as well as the constant term) will be the same as for $P(\omega)$ in [1]:

$$\sum_{n=1}^{N_d} \phi_n^2(x) + \sum_{k=1}^{N_b} \psi_k(x)[\psi_k(x) + \mu_0 \psi_k(y)].$$

  Therefore, one can again expect to observe a "catastrophic" event when this term is equal to zero.
- The multiplication of the determinant by $i\omega$ means that the terms with an even power of ω become of odd power and vice versa. It was mentioned in [1, Section 3], that by multiplying quadratic polynomials of the form $-\omega^2 + 2i\omega_n\delta_n\omega + \omega_n^2$, the terms of odd powers are linear combinations of damping factors, whereas the terms of even powers are combinations of products of natural frequencies (plus products of damping factors which are negligible in general). This implies that in practice, the odd power coefficients are in general about a hundred times lower in magnitude than those of even power. When multiplied by $i\omega$, the roles are switched, so that the addition of the determinant term to the $D(\omega)$ amounts to: (1) adding relatively small quantities to the coefficients of even power of the polynomial coming from D, which should be of little effect in general, and (2) adding relatively large values to the coefficients of odd power of the polynomial coming from $D(\omega)$. This can be interpreted as introducing a form of damping: P_ε would have odd power terms, even though the two subsystems were structurally undamped (i.e., $\delta_i = 0$). This confirms the close relationship between a coefficient of friction varying with sliding speed and damping. The validity of this argument is strongly dependent on the actual value of the product εN_0. This point will be discussed further in the next section.

Finally, note that although the combinations of mode shape coefficients appearing in the determinant are all positive, the complex analysis argument used in [1, Section 3] is unlikely to hold for at least two reasons: (1) the various terms appearing in E have a different nature: some have a single quadratic denominator, some have the product of two quadratics; (2) even if the mode shape combinations are all positive, the determinant is multiplied by *minus* $i\omega$, so that the final result could still contain negative signs if ε is positive. Therefore, instability might occur, even if the brake mode shape combinations, $\psi_n(x)[\psi_n(x) + \mu_0\psi_n(y)]$, are all positive. Whether this is the case or not will be revealed by simulations. Before investigating the behaviour of a generic system, it is useful to examine the orders of magnitude of some of the terms appearing in Eq. (16).

4.2.3. Estimation of orders of magnitude

The behaviour of a system comprising a limited number of modes will be simulated, using the new criterion (16), derived from the more sophisticated friction law (9). To use plausible values for the disc modal amplitudes, $\phi_n(x)^2$ and $\phi_n(y)^2$, it is necessary to estimate the relative orders of magnitude of these two quantities. To this end, the values of these modal amplitudes were computed using analytical expressions obtained from an annular thin plate model for a disc of comparable dimensions to a typical vehicle brake disc. From this calculation, it appears that, at least for the lowest modes (zero or one nodal circle), $\phi_n^2(x)$ ranges from 1 to 10, more frequently

around 10. $\phi_n^2(y)$ is often of order 10^{-3} and sometimes smaller. For the brake, there is no reason to believe that, in general, there should be such a difference in magnitude between H_{11} and H_{22}. It is now possible to examine expansion (18), bearing these orders of magnitude in mind.

As already mentioned, it is very difficult to estimate the values of ε and N_0, as those two parameters may strongly depend on the specific system implementation. However, using a simple order-of-magnitude analysis, it possible to estimate a critical value of the product εN_0. $E(\omega)$ appears as the combination of two different terms, the first of which is the function $D(\omega)$, the second is $i\varepsilon N_0 \omega \det[\mathbf{H}+\mathbf{G}]$. The magnitude of $D(\omega)$ can be taken as the peak amplitude of a transfer function:

$$\frac{a}{\omega^2\delta},$$

where a denotes the amplitude, ω the natural frequency and δ the corresponding damping factor. Similarly, the order of magnitude of the second term can be approximated by

$$\varepsilon N_0 \omega \frac{a^2}{\omega^4\delta^2}.$$

The ratio of these two orders of magnitude should provide a rough estimate of the value of εN_0 for which the second term becomes significant compared to the first one. Dividing the two terms yields:

$$\frac{\varepsilon N_0 a}{\delta\omega}. \tag{20}$$

A value of order unity for this ratio defines the critical value of εN_0. If $\varepsilon N_0 \ll \delta\omega/a$, one expects the system behaviour to be similar to that described in the companion paper [1]. Conversely, if $\varepsilon N_0 \gg \delta\omega/a$, the new term introduced should have a significant influence, altering the behaviour previously described.

Throughout this paper and its predecessor [1], damping has been assumed to be light, (i.e., $\delta \sim 0.01$). It was shown that a was typically equal to 10, and frequencies were normalized so that the ratio (20) is of order 0.001. If N_0 takes the plausible value of 100 N, the critical value of ε is 10^{-5}. This very small value is partly due to the natural frequency normalization. For a frequency of about 1 kHz, the critical value of ε would be 0.01. This is still fairly small, suggesting that a very slightly varying coefficient of friction could have a significant effect on the system stability.

4.3. Study of a generic system

In this section, the behaviour of a three-mode system is investigated, using the new stability criterion (16). The method used to explore this system will be the same as in the previous cases: two modes, say of the disc, will be kept fixed, while a third one, from the brake, will be varied in "amplitude" and frequency. In the companion paper [1], the "amplitude" parameters, $a_1 = \phi_1^2(x)$, $a_2 = \phi_2^2(x)$, $a_3 = \psi(x)[\psi(x) + \mu_0\psi(y)]$, were independent. As can be seen from Eq. (18), it is no longer possible to group the mode shape combinations into single parameters "a_n", because each mode shape coefficient appears in several places. Therefore, instead of varying a whole compound like a_n, mode shape coefficients ($\phi_n(x), \psi_k(y)$, etc...) will be varied individually. This raises the issue of finding plausible values for each of them. For the disc, the mode shape estimations from

Section 4.2.3 can be used directly. They were given the following values:

$$\phi_1(x) = \phi_2(x) = 3 \quad \text{and} \quad \phi_1(y) = \phi_2(y) = 0.05, \tag{21}$$

so that $\phi_{1/2}^2(x) \sim 10$ and $\phi_{1/2}^2(y) \sim 10^{-3}$. For the brake, it is difficult to estimate which values the mode shape coefficients should be given in comparison to those of the disc. There is probably no correlation between the magnitude of the mode shape coefficients of the two subsystems in general, but a conclusion from the companion paper [1] is that strong instability occurs when the leading coefficient of P_ε is around zero. For this condition to be satisfied, $\psi(x)[\psi(x) + \mu_0\psi(y)]$ must be equal to $-(\phi_1(x) + \phi_2(x)) = -18$. This value is reached when $\psi(y) = -17$. For comparison with the previous analysis, the ψ-compound should be varied from about -50 to 0. However, it was mentioned that instability could arise, even if all the "mode shape compounds" are positive. Therefore, the range of variation is extended to positive values, say 50 as well. If $\mu_0 = 0.5$, and if $\psi(x)$ is set to 4,

$$-50 \leqslant \psi(x)[\psi(x) + \mu_0\psi(y)] \leqslant +50 \quad \text{is equivalent to} \quad -33 \leqslant \psi(y) \leqslant +18.$$

For the simulation described next, the two fixed modes have frequencies $\omega_1 = 1$ and $\omega_2 = 1.2$ and the same damping factors $\delta_1 = \delta_2 = 0.01$. The brake mode frequency, ω_3 is varied from 0.8 to 1.4, and its damping factor is 0.03. Following the same format as before, Fig. 4 shows

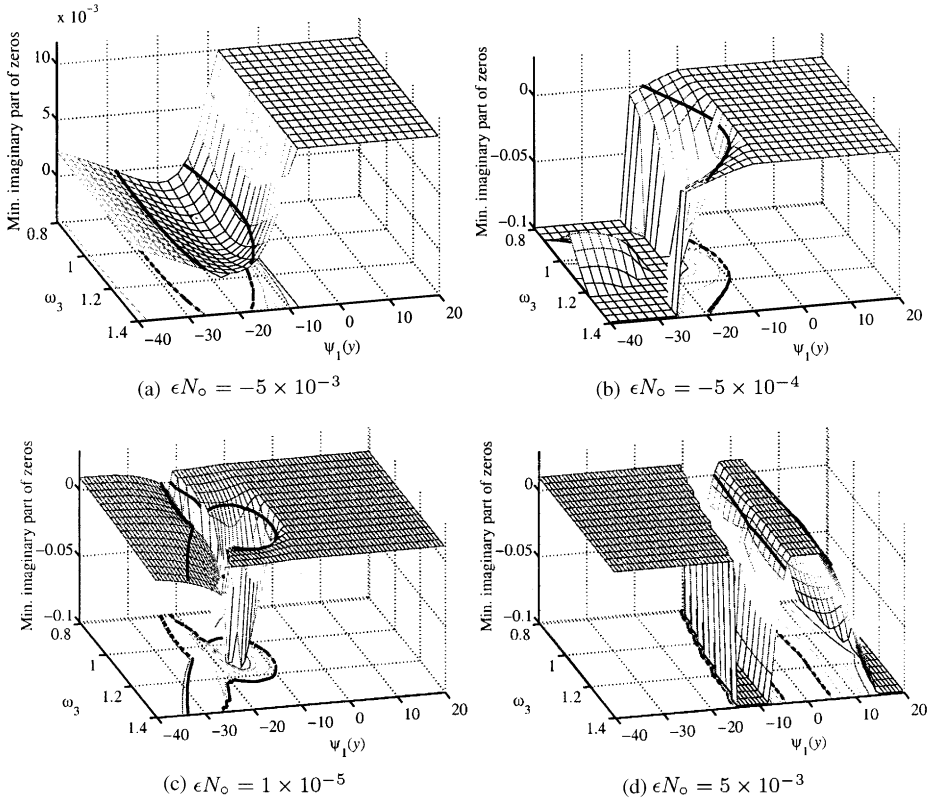

Fig. 4. Surface plots showing the minimum imaginary part of the zeros for four different values of εN_0. The underlying system consists of three modes.

surface plots of the minimum imaginary part of those zeros of $E(\omega)$ whose imaginary parts lie within 0.6 and 1.6. Each plot corresponds to a different value of εN_0, everything else being unchanged.

For each plot, the zero contour is shown with a thick line on the surface and on the bottom plane. Note that the surface has been clipped only when it reaches fairly large negative values. This does not occur in Fig. 4(a), therefore the vertical scale is different from the other plots. These plots show that a linearly varying coefficient of friction can have a strong effect on the stability of this system. Several observations can be made:

(1) Fig. 4(a) shows that when εN_0 is sufficiently large and negative, an otherwise unstable system can be stabilized. This is in accordance with the common belief that a coefficient of friction increasing with sliding speed can stabilize an otherwise unstable system. (See the preliminary remarks for the relation between the sign of ε and the slope of the μ against sliding velocity curve.)

(2) Conversely, for relatively large and positive values of εN_0 (Fig. 4(d)), the system is unstable within two narrow bands, almost independent of ω_3, and roughly symmetrically located around the plane $\psi(y) = 0$. The effect is not as strong as one could have expected from a "negative resistance". Instability is now possible even if the brake mode shape combination is positive. This possibility was mentioned in the previous section. As ε is increased (up to 0.1, case not shown), the two bands become narrower and they tend to conflate. This would suggest that higher values of ε do not make the stability of the system worse.

(3) Fig. 4(c) is very similar to the surface plot obtained for the same underlying system with a constant coefficient of friction. It is reassuring that for small values of ε, the previous case is recovered. Fig. 4(c) can be thought of as a transition case. Other simulations show that plots such as Fig. 4(c) are obtained for any value of εN_0 within $[-10^{-4} \ +10^{-5}]$. This confirms that $\varepsilon N_0 \sim 10^{-3}$ is indeed a critical value, a conclusion from the order-of-magnitude analysis in the previous section.

(4) As εN_0 becomes relatively large, either positive or negative (e.g., Fig. 4(a)(d)), it appears that the dependence of the surface with ω_3 is somehow obliterated, so that the surface plots show hardly any variation along the frequency axis. Other simulation results confirm this observation although the reason why this should be the case is not clear.

(5) Interestingly, even for relatively large values of εN_0 (e.g., Fig. 4(a)(d)), the magnitude of the minimum imaginary part is still of the order of a typical damping factor δ. This does not seem to support the argument from the previous section, according to which large values of ε make the odd power coefficients of P_ε significantly bigger, so that the imaginary parts of the roots should become larger too. Inspection of the individual behaviour of the roots shows that one of them has indeed a comparatively large imaginary part. However, this is not apparent on the surface plot because the corresponding real part is outside the range of validity. Interestingly, the magnitude of the imaginary part of the other roots is still governed by the damping factors. This is a reminder of the fact that the relationship between the odd-power coefficients of a polynomial and the imaginary part of its roots is not straightforward.

4.4. *Influence of a complex* ε

Although this section has been phrased in terms of a coefficient of friction varying with sliding speed, a friction law such as Eq. (12) can actually describe a much broader class of constitutive

friction laws, provided they can be linearized. Then, ε can no longer be interpreted as the slope of the friction–velocity curve, but it is simply the coefficient of proportionality accounting for the linear variation of F with N around a given operating point. If ε is real, as has been assumed so far, then F and N are always in phase or out of phase. This is not always the case. For example, with different contacting materials, it is possible that the interfacial temperature becomes the key parameter governing the relation between F and N [20]. In this case, thermal inertia of the contacting material creates a phase lag between the variations of F and N. This behaviour characteristically appears as a hysteresis loop in a $F-N$ plot. Such a feature could be included within our present formulation by allowing ε to be complex. The $F-N$ plot would then describe an ellipse. Simulation results not shown here suggest that, for the system studied in this section and $|\varepsilon| = 5 \times 10^{-3}$ (Fig. 4(d)), the system becomes more unstable for phase angle between 160° and 170°.

4.5. Conclusion on the influence of a varying coefficient of friction

In this section, the theory presented in the companion paper [1] was modified by coupling the two linear subsystems through a friction law featuring a coefficient of friction varying linearly with the sliding speed. This proved to modify significantly the conclusions reached with a constant coefficient of friction. To allow comparison with previous results, the influence of the new law was investigated by simulating the behaviour of the same three-mode system as before. Two modes were fixed, while the third, originating from the brake, was allowed to vary in natural frequency and tangential mode shape. The main conclusions from this study are that with such a constitutive law, this system can exhibit three different kinds of behaviour according to the magnitude and sign of the product εN_0. If this product is negative, this investigation confirms that the system tends to be stabilized, the more so, the larger $|\varepsilon N_0|$. If $|\varepsilon N_0|$ is lower than some critical value, which can be estimated by a simple order-of-magnitude analysis, the system behaves as if the coefficient of friction were constant. Therefore, in this case, the observations made in the companion paper [1] apply. If εN_0 is larger than the critical value, the system behaviour changes and becomes unstable within regions previously stable. In particular, the system can even be unstable for positive values of the brake tangential mode shape, $\psi(x)$. This was shown to be impossible with a constant coefficient of friction. However, previously unstable regions can be stabilised too, so that the influence is non-systematic and hard to predict without detailed calculations. The critical value for εN_0 turns out to be very small for the system investigated, suggesting that a slightly varying coefficient of friction can have drastic consequences on the stability. However, this small value is partly due to the chosen frequency normalisation. Finally, note that introducing a varying coefficient of friction makes the system stability depend on the operating value of the normal load N_0. In effect, increasing the value of N_0 has the same effect as increasing ε.

5. Conclusion

In this paper the modelling presented in a companion paper [1] was generalized by extending the initial formulation in three different directions. Together with [1], this paper presents an

exhaustive study of all possible routes to instability of systems comprising a single contact point, within the scope of linear theory.

First, the influence of contact springs at the interface point was studied. The reason for introducing this feature is mainly that it is a common computational device, used by researchers working with the finite element method. The results suggest that, to a good approximation, a contact compliance has a similar influence to that of a remote mode. An order of magnitude analysis showed that a compliant contact is expected to have a perceivable influence on stability if the contact spring stiffness is of the order of magnitude or below the average contact stiffness of the system.

Second, the influence of non-proportional damping was investigated. To our knowledge this is the first time this effect is mentioned in the literature as a route to instability for systems with friction. Formulating the problem in terms of transfer functions makes the study of the effect particularly simple. It was shown that a very small amount of non-proportionality can have drastic consequences on the stability. In particular, it can cause the system variables to undergo a (real) exponential growth.

Finally, the coefficient of friction was allowed to vary linearly with the sliding speed. This also proved to have a strong effect on the system stability. The well-known result that a coefficient of friction decreasing with sliding speed can destabilize a system, whereas a coefficient of friction increasing with sliding speed can only stabilize it, is certainly valid for a single-degree-of-freedom system. However, simulation results shown in this paper suggest that the effect of a varying coefficient of friction is no longer systematic for a multiple-degree-of-freedom systems. The effect is entangled with the specific pattern of sign that the mode shapes exhibit. Making the coefficient of proportionality between the coefficient of friction and the sliding velocity complex actually includes many other linearized friction laws, such as thermal or rate dependencies.

It is often argued that brake noise is an intrinsically non-linear phenomenon. It is possible that some routes to instability cannot be tackled by linear theory, but before including non-linear features in the modelling of a braking system, it seems sensible to investigate how many observed phenomena can be predicted by linear theory. By providing an exhaustive catalogue of the possible instabilities predicted by linear theory, it becomes possible to test its predictive power.

Acknowledgements

The authors thank Bosch Braking Systems for financial support and Professor K.L. Johnson for valuable discussions.

Appendix A. Nomenclature

$u_{1/2}$	displacement at the contact point on the "disc" in the normal/tangential direction
$v_{1/2}$	displacement of the contact point on the "brake" in the normal/tangential direction
F/N	total friction/normal force
F_0/N_0	average value of the friction/normal force
F'/N'	fluctuating component of the friction/normal force

$\mathbf{G}, \mathbf{H}$ (2×2) receptance matrices at the contact point for the "disc" and the "brake"
μ_0 constant coefficient of friction
ω frequency
ω_i natural frequency of mode "i"
$\bar{\omega}_i$ positive-frequency pole associated with mode "i"
δ_i damping factor of mode "i"
$\phi_i(x/y)$ mass normalized ith mode shape coefficient of the disc in the normal/tangential direction
$\psi_i(x/y)$ mass normalized ith mode shape coefficient of the brake in the normal/tangential direction
c_i residue associated with pole $\bar{\omega}_i$
ε slope of the coefficient of friction curve as a function of the sliding speed
$k_{n/t}$ stiffnesses of the contact springs in the normal/tangential directions
k_e equivalent contact stiffness

References

[1] P. Duffour, J. Woodhouse, Instability of systems with a frictional point contact. Part 1: Basic modelling, *Journal of Sound and Vibration* 271 (2004) 365–390, this issue.
[2] W.V. Nack, Brake squeal analysis by finite elements, *International Journal of Vehicle Design* 23 (2000) 236–275.
[3] K.L. Johnson, *Contact Mechanics*, Cambridge University Press, Cambridge, 1985.
[4] J.A. Greenwood, J.B.P. Williamson, Contact of nominally flat surfaces, *Proceedings of the Royal Society London, Series A* 295 (1966) 300–319.
[5] D.M. Tolstoï, Significance of the normal degree of freedom and natural normal vibrations in contact friction, *Wear* 10 (1967) 199–213.
[6] J.A.C. Martins, J.T. Oden, F.M.F. Simões, A study of static and kinetic friction, *International Journal of Engineering Science* 28 (1990) 29–92.
[7] D.P. Hess, A. Soom, Normal vibrations and friction under harmonic loads: part I—Hertzian contacts, *Transactions of the American Society of Mechanical Engineers, Journal of Tribology* 113 (1991) 80–86.
[8] D.P. Hess, A. Soom, Normal vibrations and friction under harmonic loads: part II—rough planar contacts, *Transactions of the American Society of Mechanical Engineers, Journal of Tribology* 113 (1991) 87–92.
[9] G.D. Liles, Analysis of disc brake squeal using finite element methods, SAE Paper 891150, 1989.
[10] H. Ghesquiere, Brake squeal analysis and prediction, in: *Total Vehicle Dynamics Part I*, FISITA Congress, 1992, pp. 175–181.
[11] H. Ouyang, J.E. Mottershead, M.P. Cartmell, D.J. Brookfield, Friction-induced vibration of an elastic slider on a vibrating disc, *International Journal of Mechanical Science* 41 (1999) 325–336.
[12] J.-W. Liang, B.F. Feeny, Dynamical friction behaviour in a forced oscillator with a compliant contact, *Transactions of the American Society of Mechanical Engineers, Journal of Applied Mechanics* 65 (1998) 250–257.
[13] K.L. Johnson, The contribution of micro/nano-tribology to the interpretation of dry friction, *Proceedings of the Institution of Mechanical Engineers, Part AD* 214 (2000) 11–22.
[14] W. Soedel, *Vibration of Shells and Plates*, Marcel Dekker, New York, 1981.
[15] R.E.D. Bishop, D.C. Johnson, *The Mechanics of Vibration*, Cambridge University Press, Cambridge, 1960.
[16] J. Woodhouse, Linear damping models for structural vibration, *Journal of Sound and Vibration* 215 (1998) 547–569.
[17] D.J. Ewins, *Modal Testing: Theory and Practice*, Research Studies Press, Letchworth, 1984.
[18] F.P. Bowden, D. Tabor, *The Friction and Lubrication of Solids*, Oxford University Press, Oxford, 1956.
[19] J.P. Den-Hartog, *Mechanical Vibrations*, Dover Books Reprint, New York, 1984.
[20] J.H. Smith, J. Woodhouse, The tribology of rosin, *Journal of Mechanical Physics in Solids* 48 (2000) 1633–1681.